Particle Migration in Shear Fields

C. D. DENSON, E. B. CHRISTIANSEN, and D. L. SALT
University of Utah, Salt Lake City, Utah

The motion of a single rigid sphere entrained in a glycerine-water solution flowing downward through a cylindrical tube has been investigated throughout a range of particle Reynolds numbers of 6.0 to 120.0, tube Reynolds numbers of 208 to 890, and particle-to-tube diameter ratios of 0.120 to 0.190. Trajectories of the sphere, calculated for various particle Reynolds numbers by using the Rubinow-Keller expression for the transverse force, were found to agree satisfactorily with experimentally determined trajectories when the particle Reynolds number was below 40.0. In all cases the sphere was observed to migrate to the axis of the tube. At the lower particle Reynolds numbers the sphere approached the axis asymptotically, whereas at the higher particle Reynolds numbers the sphere oscillated across the axis of the tube one or more times during migration. All observations were made with spheres which were less dense than the fluid, the density difference being as high as 10% of the fluid density.

Particle migration in a shear field refers to that phenomenon in which particles entrained in a flowing fluid move across fluid streamlines as a consequence of fluid dynamic forces. In systems where numerous particles are entrained in the fluid this phenomenon is frequently referred to as the *tubular pinch effect* or *sigma effect* (*20*); the transport of solid particles by fluids through pipelines and the determination of suspension viscosity by the capillary tube technique (*6, 13, 23* to *25*) are examples where this effect is known to occur. Although the majority of the processes where migration is an important factor involve multiparticle suspensions, research on single particle systems is a logical place to start toward gaining a better understanding of the more complicated systems referred to above. The research reported in this paper is concerned with migration of a single rigid sphere entrained in a straight tube of circular cross section.

All of the previous research on particle migration (*5, 9, 10, 12, 15, 16, 21, 27*) have been conducted within a particle Reynolds number range where fluid inertia effects were small and, with two exceptions (*9, 16*), under circumstances where the particle and fluid were closely matched in density. While all reported theoretical solutions to this problem (*1, 2, 17* to *19*) have shown that no transverse force results unless the inertial terms are retained in the Navier-Stokes equations, none of these solutions—by virtue of the techniques used to obtain the solutions—have considered inertial effects where these effects were quite large.

Because the effect of fluid inertia on a sphere entrained in a Poiseuille flow field had not been previously studied in a systematic manner, an investigation was initiated to study migration in a particle Reynolds number range where the fluid inertia effects would be larger than in previous studies; the results of this work are summarized in this paper. In this investigation the Rubinow-Keller relation was used to derive an expression for the trajectory of the sphere* and this expression was compared with trajectory data obtained experimentally. These data were obtained throughout a particle Reynolds range of 6.0 to 120.0, a tube Reynolds number range of 208 to 890, and a particle-to-tube diameter ratio range of 0.120 to 0.190. In all experiments the sphere was less dense than the fluid. It was released from rest at the wall of a tube into a downward flowing fluid at a position downstream from the entrance region.

HISTORICAL BACKGROUND

The first reported qualitative studies conducted on the motion of a solid sphere contained in a moving liquid were made by Vejlens (*27*) in 1938. His apparatus consisted of a square conduit through which an oil flowed at a tube Reynolds number of the order 2.0; the particle and entraining fluid were density matched. Vejlens found that large particles moved from the wall at a faster rate than did smaller ones; he also noted that the particles rotated as they migrated.

Segre and Silberberg (*21*) performed experiments on the behavior of dilute suspensions of rigid spheres in a Poiseuille flow field for cases where sphere density and fluid density were identical. They found that the spheres,

C. D. Denson is with General Electric Research and Development Center, Schenectady, New York.

* A theoretical expression for the transverse force on a sphere has also been derived by Saffman (*19*). Because Saffman's results were not published before this work was completed, his relation could not be compared with the results of the work reported in this paper.

while being transported through the tube, concentrated in an annular ring located at a distance about 0.6 of the tube radius from the axis, irrespective of the radial position at which the spheres first entered the tube. Spheres entering the tube near the wall migrated inward; those entering near the axis migrated outward. At tube Reynolds numbers below 30, where this effect was sharp, resulting particle Reynolds numbers were less than 6×10^{-2}. In the experimental arrangement of these investigators, the particle entered the tube with the entraining fluid. As a result, the particle was initially carried down the tube by a fluid whose velocity profile was developing. This condition may have influenced to some extent the behavior of the particle noted by Segre and Silberberg.

Particle behavior in Poiseuille flow fields has also been studied by Goldsmith and Mason (*5*). Using spheres both equal to and more dense than the entraining liquid, Goldsmith and Mason observed that although the particles rotated, they did not migrate when the particle Reynolds number was less than 10^{-6} and the tube Reynolds number was less than 2×10^{-2}. In a later work, when the particle Reynolds number was increased to 10^{-3}, Karnis, Goldsmith, and Mason (*10, 12*) observed outward migration to a radial position of 0.50. The extremely low particle Reynolds number in the former work is the reason given by these investigators for not having observed migration.

Karnis, Goldsmith, and Mason also studied the migration of a sphere in a viscoelastic liquid whose velocity gradient was zero in the central core of a cylindrical tube and nonzero close to the wall. These observations revealed that a particle entering the tube near the wall rotated and migrated until it reached the radial position where the velocity gradient was zero; at this point rotation and migration ceased. They also observed that the rate of migration increased with increased flow rate and particle size.

Oliver (*15*) measured the equilibrium radial position attained by a sphere placed in a Poiseuille flow field when the sphere was released from positions in contact with the wall and close to the axis of the tube; the tube Reynolds numbers were in the range 100 to 500 and the particle Reynolds numbers in the range 1.0 to 13.0. He observed that particles placed near the axis rotated while migrating outward and those placed near the wall rotated while migrating inward. Equilibrium was attained at a distance of 0.50 to 0.65 tube radius from the axis. Oliver's results, however, may also have been influenced by the fact that at the higher particle Reynolds numbers his observations were made on a particle entrained in a fluid whose velocity profile was not fully developed. In addition to the above set of experiments Oliver also performed experiments wherein the particle was restrained from rotating. Under these conditions, he again observed migration, concluding that rotation causes migration away from the tube axis, while short-range hydrodynamic forces cause migration away from the wall.

Most recently, studies on particle migration have been conducted by Repetti and Leonard (*16*) and by Jeffreys and Pearson (*9*). Repetti and Leonard investigated the motion of a rigid sphere at low particle Reynolds numbers when the sphere was entrained in a fluid flowing downward in a tube of rectangular cross section. They found that when the density difference between the sphere and fluid was within 0.1% of the fluid density, the sphere migrated in one of three ways: (1) from the wall of the tube to the axis of the tube; (2) from the axis to the wall; (3) or to an annular region midway between the tube wall and tube axis.

Jeffreys and Pearson studied the motion of a rigid sphere entrained in a fluid flowing in a vertical tube of circular cross section when the flow was laminar. For cases in which the sphere and fluid were density matched it was found that the sphere migrated into a narrow annular ring; on the other hand, when the particle was slightly more dense than the fluid, the particle migrated to the wall for a downward flowing fluid and to the axis for an upward flowing fluid. These observations were made within a tube Reynolds number range of 10 to 200, a particle-to-tube diameter ratio range of 0.05 to 0.10, and a range of 0 to 0.2 for the ratio of the Stokesian free fall velocity to the maximum fluid velocity.

Theoretical efforts to explain particle migration have been made by Brenner and Happel (*1*), Rubinow and Keller (*17*), and Saffman (*19*). Brenner and Happel solved the linearized Navier-Stokes equations for flow around a sphere in a Poiseuille flow field. Although their solution did not reveal the existence of a transverse force, the solution did show that when the particle-to-tube diameter ratio was small:

1. The relative velocity that should be used in calculating the particle Reynolds number and the drag force on the sphere is

$$\vec{z} = \vec{u'} - \vec{V}_o\left(1 - \frac{b^2}{R_o^2}\right) + \frac{2}{3}\left(\frac{a}{R_o}\right)^2 \vec{V}_o \tag{1}$$

2. The particle is caused to rotate by a torque whose magnitude is

$$\vec{T} = 8\pi\,\mu a^3 \frac{V_o b}{R_o^2} \vec{\lambda}_\theta \tag{2}$$

These results are identical with those obtained by Simha (*22*).

In contrast to the work of Brenner and Happel, Vand (*26*) solved the linearized Navier-Stokes equations for a large sphere situated near the wall of a tube through which a fluid was flowing under laminar conditions. Vand found that the torque on the particle is given by

$$\vec{T} = 8\pi\mu a^3 \frac{V_o b}{R_o^2}\phi\,\vec{\lambda}_\theta$$
$$\phi = \left[1 + \frac{5}{16}\frac{\left(\frac{a}{R_o}\right)^3}{\left(1 - \frac{b}{R_o}\right)^3} + \ldots\ldots\right]^{-1} \tag{2a}$$

This equation was subsequently given experimental verification by Goldsmith and Mason (*5*).

Rubinow and Keller (*17*) solved the Navier-Stokes equations, inertia terms retained, for the case of a spinning sphere travelling with a constant velocity u' through a stagnant unbounded fluid. Their solution revealed that if a particle is caused to rotate, then a transverse force is developed; the magnitude of this force is

$$\vec{F}_T = \pi a^3 \rho_f \vec{\omega} \times \vec{u'} \tag{3}$$

In addition, the rotation of the particle is resisted by a torque whose magnitude is

$$\vec{T} = -8\pi\mu a^3 \vec{\omega} \tag{4}$$

Finally, the drag force on the sphere was found to be

$$\vec{F}_D = -6\pi\,\mu a\,\vec{u'}\left(1 + \frac{3}{16}N_{Re_p}\right) \tag{5}$$

which is identical to the expression for drag derived by Oseen.

Most recently Saffman (*19*) has derived an expression for the transverse force on a sphere entrained in fluid moving with uniform simple shear. He found that the transverse force is independent of the rotation of the sphere and is given by

$$\vec{F}_T = 81.2\, a^2 \vec{\dot{z}}\, (\Gamma \mu \rho_f)^{1/2}$$

TRAJECTORIES FROM THEORY

An analytical expression for the trajectory of a migrating particle can be obtained by applying Newton's second law of motion

$$m[\vec{a}] = \Sigma \vec{F} - m\ A_o \tag{6}$$

$$I \vec{\alpha} = I \frac{d\vec{\omega}}{dt} = \Sigma \vec{T} \tag{7}$$

to a solid spherical particle moving with a time-variant velocity $\dot{b}\, \vec{\lambda}_r + u' \vec{\lambda}_k$ through a fluid flowing in a circular tube. Figure 1 is a sketch of this system. Because the case of a fluid in laminar flow is being considered, the velocity profile of the fluid will be of the form $\vec{V}_o \left(1 - \frac{r^2}{R_o^2}\right)$. In addition, for the sake of convenience, a moving reference frame whose velocity is

$$\vec{u}'' = \left[V_o \left(1 - \frac{b^2}{R_o^2}\right) - \frac{2}{3} \left(\frac{a}{R_o}\right)^2 V_o \right] \vec{\lambda}_k \tag{8}$$

will be chosen. Further, let it be assumed that:

1. The square of the ratio of the particle's radial component of velocity to its axial component of relative velocity is much less than unity.
2. The drag force on the particle is not affected by the spin of the particle.
3. Equation (4), the expression for the resisting torque, is valid for an angularly accelerating particle.

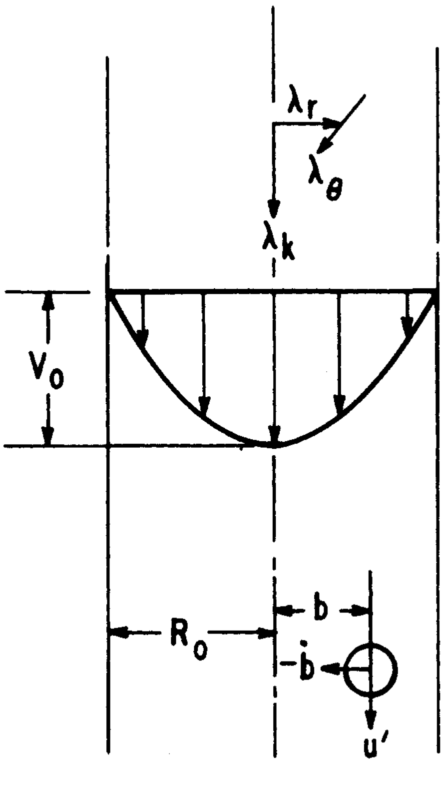

Fig. 1. Sphere in a Poiseuille field.

4. Little error is introduced in the analysis by using, as a first approximation, the well-known steady state drag coefficient curve for calculating the translational drag force, even though the spinning particle has a rectilinear acceleration.
5. The Rubinow-Keller result, although derived for a sphere undergoing steady motion, can be applied to a sphere undergoing unsteady motion.
6. The Rubinow-Keller result, although derived for a sphere caused to rotate by an external agency, is equally valid when the external agency is a shear field.

These assumptions and the limitations which they impose on the analysis are discussed below.

The derivation proceeds by substituting into Equation (6) the forces which act on the particle during migration

$$\Sigma \vec{F} = \vec{F}_T + \vec{F}_B + \vec{F}_D \tag{9}$$

where

$$\vec{F}_T = \pi a^3 \rho_f \vec{\omega} \times [\dot{b}\, \vec{\lambda}_r + \dot{z}\, \vec{\lambda}_k]$$

$$\vec{F}_B = (\rho_s - \rho_f)\, V_p\, \vec{g}$$

$$\vec{F}_D = \frac{C_D \rho_f A_p}{2} (\dot{b}^2 + \dot{z}^2) \frac{(\dot{b}\, \vec{\lambda}_r + \dot{z}\, \vec{\lambda}_k)}{\left| \dot{b}\, \vec{\lambda}_r + \dot{z}\, \vec{\lambda}_k \right|}$$

and

$$\vec{\dot{z}} = (u' - u'')\, \vec{\lambda}_k$$

Equation (7), which expresses the relation between the rotational velocity of the particle and time, can be written in the following form by utilizing Equation (2*a*) and Equation (4):

$$I \frac{d\vec{\omega}}{dt} = -8\pi\mu a^3 \left[\omega - \frac{V_o b}{R_o^2} \phi \right] \vec{\lambda}_\theta \tag{10}$$

By writing Equation (9) in component form and by using the first assumption listed, there results

$$m\, \ddot{b} = \pi a^3 \rho_f\, \omega\, \dot{z} - \frac{C_D \rho_f A_p}{2} |\dot{z}|\, \dot{b} \tag{11}$$

$$b\, \ddot{z} = (\rho_s - \rho_f)\, V_p\, g - \pi a^3 \rho_f\, \omega\, \dot{b} - \frac{C_D \rho_f A_p \dot{z}^2}{2} - 2\, m\, V_o\, b\, \dot{b}/R_o^2 \tag{12}$$

The last term on the right-hand side of Equation (12) accounts for the acceleration of the reference frame and was obtained in the form shown by using the chain rule for differentiation.

In neither of the above equations was the drag force corrected for the presence of the walls. That such a correction is unnecessary in the present work is substantiated by the work of McNown and Newlin (*14*). The results of these investigators indicate that within the particle Reynolds number range and particle-to-tube diameter ratio range covered in the present work, this correction factor is sufficiently close to unity so that little error is introduced in the final results by neglecting the factor. On the other hand, it should be stated that McNown and Newlin's results in themselves introduce into the analysis an additional assumption, this assumption being that the drag correction for a sphere with components of motion parallel and perpendicular to the wall is identical to the correction for a particle which moves parallel to the wall only. The manner in which this latter assumption is taken into consideration in this analysis will be discussed forthwith.

Equations (10), (11), and (12) can be put in dimensionless form by defining the following quantities:

$$
\begin{aligned}
q &= \frac{b}{R_o} & Z &= \frac{L}{R_o} \\
\frac{dq}{d\theta} &= \frac{a^2\,\rho_s}{R_o\,\mu}\,\dot{b} & \frac{d\eta}{d\theta} &= \frac{a^2\,\rho_s}{R_o\,\mu}\,\dot{z} \\
\frac{d^2q}{d\theta^2} &= \frac{a^4\,\rho_s{}^2}{R_o\,\mu^2}\,\ddot{b} & \frac{d^2\eta}{d\theta^2} &= \frac{a^4\,\rho_s{}^2}{R_o\,\mu^2}\,\ddot{z} \\
\Omega &= \frac{a^2\,\rho_s}{\mu}\,\omega & \theta &= \frac{\mu}{a^2\,\rho_s}\,t
\end{aligned}
\tag{14}
$$

Substitution of these quantities into Equations (10), (11), and (12) yields

$$
\frac{d^2q}{d\theta^2} = \frac{3}{4}\,\Omega\,\frac{\rho_f}{\rho_s}\,\frac{d\eta}{d\theta} - \frac{3}{16}\,[C_D\,N_{Repz}]\,\frac{dq}{d\theta} \tag{15}
$$

$$
\frac{d^2\eta}{d\theta^2} = -\frac{\Delta\rho\,g\,a^4\,\rho_s}{R_o\,\mu^2} - \frac{3}{4}\,\frac{\rho_f}{\rho_s}\,\Omega\,\frac{dq}{d\theta} - \frac{3}{32}\left(\frac{a}{R_o}\right)\frac{\rho_s}{\rho_f}\,C_D\,N^2{}_{Repz} - 2\left(\frac{a}{R_o}\right)^2\frac{\rho_s}{\rho_f}\,N_{Re}\,\frac{dq}{d\theta} \tag{16}
$$

$$
\frac{d\Omega}{d\theta} = -15\left[\,\Omega - \left(\frac{a}{R_o}\right)^2\frac{\rho_s}{\rho_f}\,N_{Re}\,\phi\,\right] \tag{17}
$$

$$
\frac{dZ}{d\theta} = \frac{d\eta}{d\theta} + \left(\frac{a}{R_o}\right)^2\frac{\rho_s}{\rho_f}\,N_{Re}\,(1-q^2) - \frac{2}{3}\left(\frac{a}{R_o}\right)^4\frac{\rho_s}{\rho_f}\,N_{Re} \tag{18}
$$

Equation (18) in the above set was included to transform the solution to a stationary reference frame.

Equations (15), (16), (17), and (18) were solved by means of an Electronic Associates analog computer by using as initial conditions: (1) the radial position of the particle in the tube q; (2) the radial velocity of the particle $dq/d\theta$; (3) the angular velocity of the particle Ω; (4) the axial position of the particle Z; and (5) the axial component of the relative velocity $d\eta/d\theta$. Coefficient-setting potentiometers were used to read into the computer the coefficients in the differential equations. The resulting solutions are presented as the solid curves in Figures 2 and 3.

A semiquantitative estimate of the sphere's trajectory can be obtained by writing Equation (11) in the form of Equation (11*a*) and by asuming that the rotational velocity of the particle is equal to one-half the curl. Hence

$$
\vec{\omega} = \frac{1}{2}\,\nabla\times\vec{u} = \frac{V_o b}{R_o{}^2}\,\vec{\lambda}_\theta
$$

Therefore

$$
m\ddot{b} + c\dot{b} + kb = 0 \tag{11a}
$$

where

$$
c = \frac{C_D \rho_f A_P}{2}\,|\dot{z}|
$$

$$
k = \pi a^3 \rho_f\,\frac{V_o}{R_o{}^2}\,|\dot{z}|
$$

Under circumstances when the axial component of the relative velocity is constant, or nearly so, Equation (11*a*) is seen to be identical to the equation which describes the motion of a mass attached to a spring and dashpot (*4*). Therefore, in the present study, one would expect the sphere to approach the equilibrium position in an asymptotic manner or an oscillatory manner, depending on whether 4 mk is less than or greater than c^2. In the discussion which follows it will be seen that this type of behavior was experimentally observed.

DISCUSSION OF ASSUMPTIONS

The first assumption used in deriving the differential equations was made primarily to make the equations somewhat more tractable. This assumption was found, from the experimental data taken as part of this study, to be valid for values of the particle Reynolds number below 40.0. For example, at a particle Reynolds number of 35.0, the square of the ratio of the particle's radial component of velocity to its axial component of velocity was found to be 0.06, at a particle Reynolds number of 45.0 to be 0.25, and at a particle Reynolds number of 60.0 to be 0.40.

With respect to the second assumption the theoretical work of Brenner and Happel (*1*) and Rubinow and Keller (*17*) have shown that the drag force is unaffected by particle spin at relatively low particle Reynolds numbers; however, the range of particle Reynolds numbers over which these analyses are valid is largely unknown at the present time due to the lack of experimental data. If within the range of particle Reynolds numbers covered in the work reported in this paper an interaction between the drag force and particle spin exists, then large errors could be introduced in the present analysis.

The third assumption, that the torque expression is unaltered by the fact that the particle may have an angular acceleration, is believed to have little effect on the solution when the rate of rotation is low. On the other hand, the magnitude of the rotational particle Reynolds number $2a^2\omega\rho/\mu$ may be in a range where the resisting torque is not linearly related to the rotational velocity of the par-

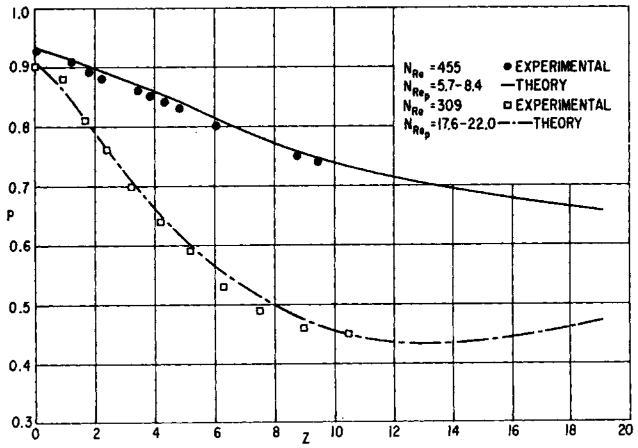

Fig. 2. Dimensionless radial position vs. dimensionless axial position.

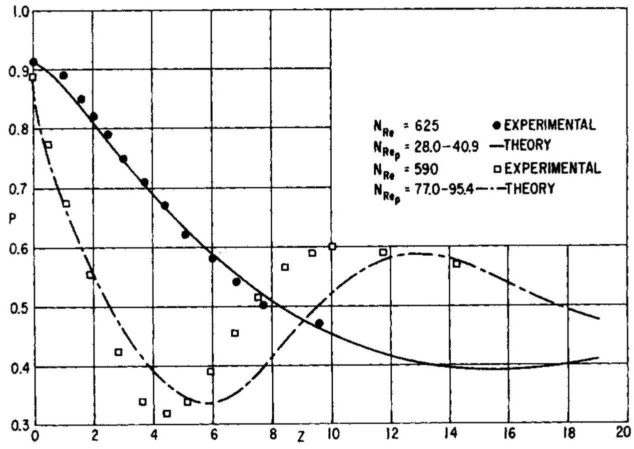

Fig. 3. Dimensionless radial position vs. dimensionless axial position.

ticle. Here again, the lack of experimental data precludes the use of any equation other than Equation (2*a*) for calculating the resisting torque.

The effect of rectilinear acceleration on the translational drag force for a spinning sphere has not been studied in any detail up to the present time. In an effort to determine how the drag force had to be corrected for this and the other effects stated above, drag coefficients were calculated from the experimental data. It was found that these drag coefficients were less than those given by the steady state drag coefficient curve at identical particle Reynolds numbers. In fact, these drag coefficients were found to agree quite closely with those determined by Ingebo (7, 8) for an accelerating sphere. By virtue of this latter result, all theoretical solutions were computed by using drag coefficients calculated from the data obtained in this study, in lieu of the drag coefficients given by the steady state curve.

EXPERIMENTAL

In order to determine the validity of the theoretical trajectories—the solutions to the differential equations derived above—experimental trajectories were obtained for a single rigid sphere entrained in a Poiseuille flow field. These data were then compared with the theoretical solutions.

In all experiments the sphere was released from rest at the wall of a glass tube of cylindrical cross section; the fluid, a glycerine-water solution, flowed vertically downward. Attention was focused primarily on the influence exhibited by two variables on particle trajectories. The first of these, the tube Reynolds number, was varied over a range of 208 to 890 by varying the composition and flow rate of the solutions used. The second of these, the particle Reynolds number, was varied over the range of 6.0 to 120.0 by varying the particle size, density difference, and fluid flow rate. By performing preliminary experiments it was found that in order for the sphere to migrate from the wall toward the tube axis, the sphere had to be less dense than the fluid. When the fluid flowed downward, spheres which were more dense than the fluid did not migrate from the wall.

The flow apparatus used for obtaining the Poiseuille velocity distribution and for observing the particle's motion was arranged such that the glycerine-water solution flowed from a feed tank, by means of a hydraulic head, downward through the glass tube. The I.D. of this tube was 1 in. The length of the tube was 7 ft.; however, only a 7-in. long section of this tube was used to observe the sphere's trajectory. The entrance to the tube, a glass bell mouth smoothly joined to the tube, was placed inside the feed tank. In order to reduce distortion due to the curved surface, the tube was enclosed in a rectangular Lucite box filled with a solution of dibutyl phthalate (60% by weight) in Ucon Oil LB1715 (5); the index of refraction of this mixture was identical to that of the glass and very nearly equal to the index of refraction of the glycerine-water solution. After passing through the tube, the solution flowed upward through a valve and a rotameter to a reservoir tank whose elevation was lower than that of the feed tank. The fluid was then returned to the feed tank by means of a small centrifugal pump. Copper coils, through which cold water was circulated, were mounted in the reservoir tank to maintain the solution at constant temperature.

The spheres, made of polyethylene and having nominal diameters of 4/32, 5/32, and 6/32 in., were electroplated with a thin layer of nickel to render them susceptible to a magnetic field. An electromagnet placed against the outside wall of the tube served as a means of releasing the particle. To insure that the velocity profile would be fully developed at the point where the particle was released, the electromagnet was placed 45 pipe diameters downstream from the entrance. Experimental measurements of the velocity profiles of the undisturbed fluid at the release point verified that a fully developed parabolic profile did exist at all tube Reynolds numbers less than 800.

Quantitative data on the trajectory of the sphere were obtained by multiple exposure photography with a 5-in. $\times$ 7-in. view camera. The camera was equipped with an 8¼-in., f/5.6 Schneider Symmar lens and an 18-in. length of bellows to provide for one-to-one magnification. Illumination of the particle was obtained by means of a xenon lamp placed at right angles to the camera. The lamp, emitting an intense beam of light, was flashed at a constant frequency during a given experiment by an Edgerton, Germeshausen, and Grier stroboscope; flashing frequencies were varied from 7 flashes/sec. for the lowest flow rate to 25 flashes/sec. for the highest flow rate. A Hewlett-Packard Square-Wave generator synchronized with a Hewlett-Packard audio oscillator served to trigger the stroboscope.

When an experimental run was to be made, weighed quantities of glycerine and water, to give a desired composition, were added together and thoroughly mixed. The density of the mixture was determined by means of a pycnometer. The density of the sphere was determined by a sink-float technique by using an aqueous sodium chloride solution of known density. The diameter of the particle, previously selected for roundness, was measured to within 10 microns by means of a Nikon Shadowgraph.

Data Reduction

The Nikon Shadowgraph was used to measure radial and axial distances from the release point to each of the images appearing on the negative. These distances were corrected for distortion by means of a function calculated from measurements of the distances between horizontal and vertical lines on a calibrated grid and from measurements of the distances between corresponding lines on a photograph taken of the calibrated grid when the grid was placed in the tube. The overall error in the reported values of the dimensionless distance between the center of the sphere and the tube wall was found to be less than 2.1% of this dimensionless distance.

Complete details on the experimental apparatus, procedure, and method of data reduction are given in reference 3.

An Illustrative Photograph

Examination of a typical photograph taken of a migrating sphere at a high particle Reynolds number revealed that upon release the particle moved toward the axis of the tube as it traveled downstream. After the particle crossed the axis it continued toward the other side of the tube, reversed direction *before* it reached the wall, and moved back toward the centerline. The particle then would cross the axis again, continue over to that side of the tube from which it was released, again reverse direction, and move back toward the axis. To determine whether the particle simply spiralled around the axis giving the impression that it had actually crossed the axis, the camera and light source were interchanged. Photographs taken of the motion of the sphere revealed that the particle did not spiral around the axis; in fact, movement in the angular direction was negligible.

Experimental data on the rotational velocity of the particle were also obtained by taking movies of a particle upon which stripes had been marked. These pictures revealed that after release the particle rotated in a direction such that its spin vector was always coincident with the direction of the curl. That is, on the right-hand side of the centerline the particle rotated counterclockwise. After the particle crossed the centerline, the direction of rotation was reversed.

DISCUSSION OF RESULTS

A few examples of the computer solutions and the experimental data obtained in this study are shown graphically in Figures 2 and 3. These graphs illustrate that the motion of the sphere in this system is similar to the motion of a mass attached to a spring-dashpot system whose behavior ranges from underdamped oscillatory to overdamped nonoscillatory motion. In the particle Reynolds number range 6.0 to 10.0 the particle was found to exhibit nonoscillatory motion, approaching the axis of the tube asymptotically. As the particle Reynolds number was increased to values between about 16.0 to 120.0, the sphere exhibited underdamped oscillatory motion, passing through the axis of the tube one or more times before migration

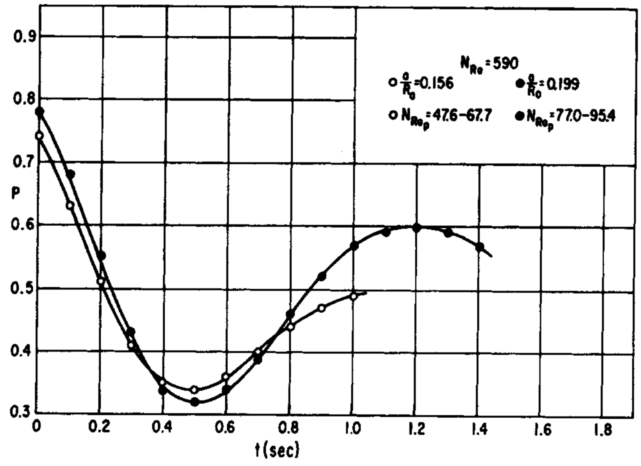

Fig. 4. Dimensionless radial position vs. time.

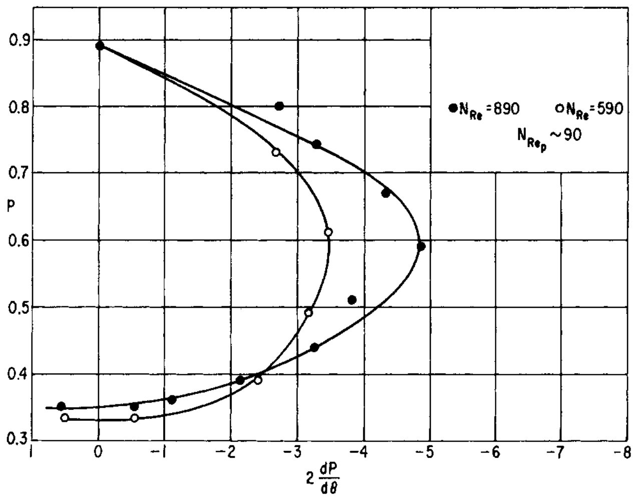

Fig. 6. Dimensionless radial position vs. dimensionless radial velocity.

ceased. The agreement between the experimental data and the analytical solutions was found to be good for values of the particle Reynolds number below 40.0, indicating that the assumptions made in the analysis are valid and do not introduce large errors. The divergence of theory and experiment above a particle Reynolds number of 40.0 is believed to be due to the fact that the unsteady effects are high (that is, the fifth assumption is invalidated) and inertial effects are large enough to introduce flows not considered in the Rubinow-Keller analysis.

When the radial position of the sphere was plotted against time for a given tube Reynolds number, it was found as exemplified by the graph in Figure 4, that the frequency of oscillation increased with increased particle Reynolds number. From this it can be concluded that the transverse force increases with increased particle Reynolds number. In addition, since the particle Reynolds number increases with increased particle size, it can also be concluded that the transverse force increases with increased particle size (a/R_o).

The effect of the fluid flow rate (tube Reynolds number) on the motion of the particle is shown in Figure 5. Although data were not taken over a complete cycle during oscillation, the half-cycle data show that the frequency of oscillation increases with increased flow rate, indicating that the transverse force increases with flow rate. One is led to the same conclusion by examining a graph of radial velocity versus radial position (Figure 6) for the runs shown in Figure 5. Since the maximum value of the radial velocity increases with increased flow rate, it can again be concluded that the transverse force increases with increased flow rate.

The rotational velocity of the particle was found from experiment to increase with increased flow rate and, at a given flow rate, to exhibit a maximum (Figure 7). The existence of the maximum can be explained by the fact that the velocity gradient of the fluid is highest at the wall and zero at the axis. When the particle is released from rest at the wall, the high velocity gradient initially acts to accelerate the particle from zero angular velocity to a finite value. Then, as the particle begins to move toward the axis, the gradient—hence the rotational velocity—decreases.

Although the equations [Equations (15 to (18)] for describing the trajectory of a migrating sphere were verified for an upward settling sphere in a downward flowing fluid, these equations are by no means restricted to this specific case. For example, inspection of Equation (11), the dimensional form of Equation (15), reveals that migration toward the axis will occur for a downward settling sphere in an upward flowing fluid. In this case, as in the case of an upward settling sphere in a downward flowing fluid, the sphere lags behind the fluid and the quantity $\dot{z}$ is negative, thereby giving rise to a transverse force directed toward the axis. For the case of an upward settling sphere in an upward flowing fluid or a downward settling sphere in a downward flowing fluid, Equation

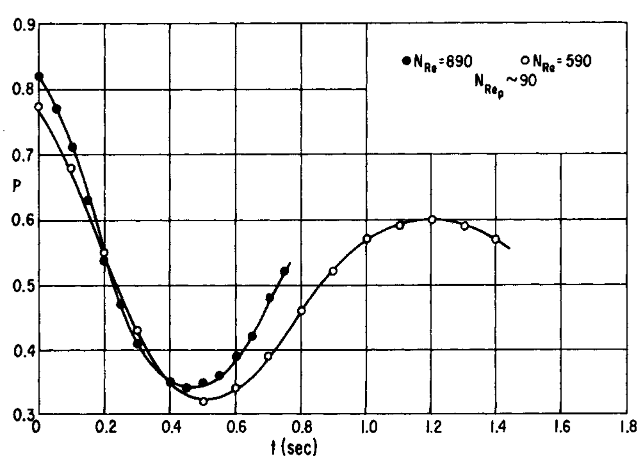

Fig. 5. Dimensionless radial position vs. time.

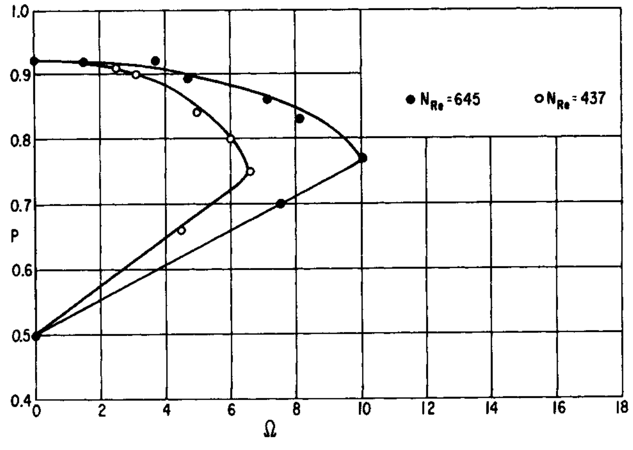

Fig. 7. Dimensionless radial position vs. dimensionless angular velocity.

(11) predicts migration toward the wall. In this instance, the sphere leads the fluid and the quantity $\dot{z}$ is positive giving rise to a transverse force directed away from the axis.

CONCLUSIONS

Based on the results of this study, it is concluded that a single rigid spherical particle entrained in a Poiseuille flow field migrates across streamlines to the axis of the tube if the particle velocity is less than the local fluid velocity. This behavior was observed over a particle Reynolds number range of 6.0 to 120.0 for the case where the particle was less dense than a downward flowing fluid. When the particle Reynolds number was low (6.0 to 10.0), the particle approached the axis of the tube asymptotically. In the particle Reynolds number range of about 16.0 to 120.0, the particle oscillated across the axis of the tube before migration ceased; the frequency of oscillation increased with increased particle size, particle Reynolds number, and tube Reynolds number. It has also been concluded that because the frequency of oscillation increases with increased particle size, particle Reynolds number, and tube Reynolds number, the transverse force also increases with an increase in these parameters. By virtue of experimental observations on the rotation of the sphere and the agreement between the experimental and theoretical trajectories, it is further concluded that migration is due to spin in the manner suggested by the Rubinow-Keller expression.

Finally, in addition to providing a means for predicting the trajectory of a sphere entrained in a Poiseuille flow field, the theoretical analysis has served to point out areas where new knowledge is needed. As suggested by the assumptions in the analysis, these areas are:

1. A study to determine the range of rotational particle Reynolds numbers over which the expression for the resisting torque, Equation (2), is valid.
2. A study to determine the correction to the translational drag force acting on a sphere which has components of motion parallel and perpendicular to the wall of a tube of circular cross section.
3. A study to determine the effect of spin on the translational drag force acting on an accelerating sphere.

ACKNOWLEDGMENT

This paper represents a summary of a doctoral thesis submitted to the University of Utah by Costel D. Denson. Appreciation is expressed to the Phillips Petroleum Company and the U. S. Office of Education for fellowship support.

NOTATION

a = radius of sphere, cm.
$[a]$ = acceleration of sphere, cm./sec.^{2}
A_o = acceleration of reference frame, cm./sec.^{2}
A_p = projected area of sphere πa^2, sq.cm.
b = distance from center of sphere to axis of tube, cm.
C_D = drag coefficient, dimensionless
C = resistance coefficient, (dyne)(sec.)/cm.
F = force, dynes
F_B = buoyant force, dynes
F_D = drag force, dynes
F_T = transverse force, dynes
g = gravitational acceleration, cm./sec.^{2}
I = moment of inertia, $8/15\ \pi a^5 \rho_s$, cm.^{5}
k = force constant, dynes/cm.
L = axial distance traveled by sphere, cm.
m = mass of particle, g.
P = dimensionless distance from center of sphere to tube wall, $P = \frac{1}{2}(1 + q)$
q = dimensionless distance from center of sphere to axis of tube
R_o = radius of tube, cm.
N_{Re_p} = particle Reynolds number, $2a\rho_f/\mu\ [\dot{b}^2 + \dot{z}^2]^{1/2}$
$N_{Re_{pz}}$ = particle Reynolds number, $(\dot{b}^2/\dot{z}^2 << 1,)\ 2a\rho_f/\mu\ \dot{z}$
N_{Re} = tube Reynolds number, $R_o V_o \rho_f/\mu$
r = radial distance from tube axis, cm.
T = torque, dyne/cm.
t = time, sec.
u = axial component of fluid velocity, cm./sec.
u' = axial component of particle velocity, cm./sec.
u'' = velocity of reference frame, cm./sec.
V_o = centerline velocity of bounded fluid, cm./sec.
V_p = volume of particle, cc.
Z = dimensionless axial position of particle
$\dot{z}$ = velocity of particle relative to moving reference frame, cm./sec.

Greek Letters

α = angular acceleration, rad./sec.^{2}
λ = unit vector
ρ_f, ρ_s = density of fluid, solid g./cc.
ω = rotational velocity, rad./sec.
Ω = dimensionless rotation velocity
θ = dimensionless time
μ = viscosity, g./(cm.)(sec.)
Γ = magnitude of velocity gradient, rad./sec.

LITERATURE CITED

1. Brenner, Howard, and John Happel, *J. Fluid. Mech.*, **4**, 195 (1958).
2. Bretherton, F. P., *ibid.*, **14**, 284 (1962)
3. Denson, C. D., Ph.D. thesis, Univ. Utah, Salt Lake City (1965).
4. Fowles, G. R., "Analytical Mechanics," Holt, Rinehart and Winston, New York (1962).
5. Goldsmith, H. L., and S. G. Mason, *J. Colloid Sci.*, **17**, 448 (1962).
6. Higginbotham, G. H., D. R. Oliver, and S. G. Ward, *Brit. J. Appl. Phys.*, **7**, 372 (1958).
7. Ingebo, R. D., *Natl. Advisory Comm. Aeronaut. Tech. Note 3265* (1954).
8. ———, *ibid.*, *3762* (1956).
9. Jeffrey, R. C., and J. R. A. Pearson, *J. Fluid Mech.*, **22**, 721 (1965).
10. Karnis, A., H. L. Goldsmith, and S. G. Mason, *Nature*, **200**, 159 (1963).
11. Magnus, G., *Ann. Phys. Chem.*, **88**, 1 (1853).
12. Mason, S. G., H. L. Goldsmith, and A. Karnis, paper presented A.I.Ch.E. Boston meeting (Dec. 6-10, 1964).
13. Maude, A. D., and R. L. Whitmore, *Brit. J. Appl. Phys.*, **7**, 98 (1956).
14. McNown, J. S., and J. T. Newlin, "Natl. U.S. Congr. Appl. Mech. Proc.," p. 801 (1951).
15. Oliver, D. R., *Nature*, **194**, 1269 (1962).
16. Repetti, R. V., and E. F. Leonard, *ibid.*, **203**, 1946 (1964).
17. Rubinow, S. I., and J. B. Keller, *J. Fluid Mech.*, **11**, 447 (1961).
18. Saffman, P. G., *ibid.*, **1**, 540 (1956).
19. *Ibid.*, **22**, 385 (1965).
20. Scott-Blair, W. G., *Rheol. Acta*, **1**, 123 (1958).
21. Segre, G., and A. Silberberg, *J. Fluid Mech.*, **14**, 115, 136 (1962).
22. Simha, R., *Kolloid-Z.*, **76**, 16 (1936).
23. Starkey, T. V., *Brit. J. Appl. Phys.*, **6**, 34 (1955).
24. *Ibid.*, **7**, 52 (1956).
25. ———, V. A. Hewlett, J. H. A. Roberts, and R. E. James, *ibid.*, **12**, 545 (1961).
26. Vand, V. J., *J. Phys. Colloid Chem.*, **52**, 300 (1948).
27. Vejlens, G., *Acta Pathol. Microbiol. Scand. Suppl.*, **33**, 159 (1938).

Manuscript received December 8, 1965; revision received March 14, 1966; paper accepted March 15, 1966.